Fourth International Colloquium on

Nonlinear Dynamics and Control of Deep Drilling Systems

Ulf Jakob Flø Aarsnes,
Nathan van de Wouw,
Emmanuel Detournay,
Vincent Denoël
Editors

Stavanger, Norway
May 14-16th, 2018

Cover Photo: Shutterstock

Foreword

This Colloquium is a follow-up of the meetings on the same topics, held at the University of Liége, Belgium, in 2009, at the Eindhoven University of Technology, The Netherlands, in 2012 and at the University of Minnesota, U.S.A., in 2014. The "control" part of the name was added at the second Colloquium to underline the two main themes.

For this Colloquium, four main domain themes were specified:

- Underbalanced Operations & Managed Pressure Drilling (UBO/MPD)

- Drill String Vibrations & Drilling Mechanics

- Geosteering & Borehole Propagation

- Drilling Automation & ROP Optimization

In keeping with the previous incarnations, however, most submissions have been focused on drill-string vibrations.

It has been the aim of the organizing committee to strive for the correct blend between industry and academia participation, and between the theoretical depth and the practical relevance of the submissions. This to ensure that the colloquium can provide an arena where the practitioners can learn what relevant theoretical tools are available, while providing feedback so as to keep the research focused and relevant to applications where it can provide value. Judging from the content of these proceedings, we believe we have succeeded in this goal. It contains both descriptions of problems encountered in the field, new developments on known problems, as well as proposing novel solutions through employment of sophisticated mathematical methods. Together, these proceedings, we truly believe, reflect the state of the art of Nonlinear Dynamics and Control of Deep Drilling Systems.

Ulf Jakob Flø Aarsnes, Nathan van de Wouw,
Emmanuel Detournay and Vincent Denoël

Acknowledgements

Program

Monday May 14
Drill String Modeling

12:00   *Lunch*

13:00   Opening

13:10   *Keynote: Is it time to start using open source models to solve drill string dynamics issues?*
Paul PASTUSEK and Greg PAYETTE

13:50   *Coffee break*

14:10   *Drill-string Dynamics in Deviated Wells in the Presence of Heave*
Eric CAYEUX

14:50   *The importance of Physics in Drill String modelling*
Bernt Sigve AADNØY and Dan SUI

15:30   *Coffee break*

15:50   *Semi-analytical models of the oil-well drillstring*
Sigve HOVDA

16:30   *High frequency torsional oscillations in BHAs: Examples and Theory*
Benjamin JEFFRYES, Zhengxin ZHANG, Yuelin SHEN, Wei CHEN, Jibin SHI, Wesley BONSTAFF, Kien TANK, David L. SMITH and Yezid AREVALO

19:00   *Dinner*

Tuesday May 15

Self excited vibrations

8:00   *Breakfast*

9:00   *State-Dependent Delay Effect in Drilling*
Xie ZHENG, Vipin AGARWAL and Balakumar BALACHANDRAN

9:40   *Effect of compression and torsion on the stability of drilling processes*
Bence BERI and Gabor STEPAN

10:20   *Coffee break*

10:40   *Improving stability of steady drilling using a non-uniform distribution of cutters on the drill-bit*
Sunit Kumar GUPTA and Pankaj WAHI

11:20   *Influence of Bit Design on the Stick-slip Vibrations of a Rotary Drilling System*
Kaixiao TIAN and Emmanuel DETOURNAY

12:00   *Lunch*

13:00   *Effectiveness Analysis of Anti Stick-Slip Tools*
Dapeng ZHAO

13:40   *Drilling experiment to determine the efficiency of a second generation downhole drilling regulator*
Nils REIMERS

14:20   *Excursion to Pulpit Rock: 7,6km with 330m altitude gain (4-5 hours) walk.*

20:00   *Dinner*

Wednesday May 16

Control of drilling systems

8:00   *Breakfast*

9:00   *Drilling Automation – Some Industrial Challenges and Solutions*
John-Morten GODHAVN and Espen Hauge

9:40   *Control-Oriented Modeling and Model Order Reduction for Managed Pressure Drilling Systems*
Sajad NADERI LORDEJANI, Bart BESSESLINK, Momhammad H. ABBASI, Glenn-Ole KAASA, Wil H. A. SCHILDERS and Nathan van de WOUW

10:20   *Coffee break*

10:40   *Performance and stability limits of distributed pressure control due to resonance caused by wave propagation*
Glenn-Ole KAASA

11:20   *Nonlinear Modeling of Directional Drilling*
Fahim SHAKIB, Emmanuel DETOURNAY and Nathan van de WOUW

12:00   *Lunch*

13:00   *Effects of latency, motor inertia and filtering on stick-slip mitigation control*
Roman J. SHOR, Ulf Jakob F. AARSNES and Florent DI MEGLIO

13:40   *Advances in control of Hyperbolic Partial Differential Equations: opportunities for drilling*
Roman J. SHOR, Ulf Jakob F. AARSNES and Florent DI MEGLIO

14:20   *Closing*

Contents

x

State-Dependent Delay Effect in Drilling

Xie Zheng, Vipin Agarwal and Balakumar Balachandran

Department of Mechanical Engineering, University of Maryland, College Park, USA

1 Introduction

Systems described by delay-differential equations arise in many science and engineering fields (i.e., networked systems, biological systems). One example in the engineering field is rotary drilling dynamics [1, 2, 3]. As shown in earlier work, the state-dependent delay can arise in the description of the cutting action of the drill bit blade on the rock interface. This delay can play an important role in determining stick-slip behavior of the system. In related previous work conducted in the authors' group, reduced-order models, finite-element based discretization, and the presence of the state-dependent delay have been discussed [3, 4]. In the current work, the authors carry out a nonlinear analysis and numerical studies with a reduced-order model to further our understanding of the state-dependent delay effect.

The remaining part of this paper is organized as follows. In Sections 2 and 3, the authors follow their earlier work reported in reference [5] and set the stage for the analyses to follow. A reduced-order model is presented to describe the axial-torsion dynamics of drilling. For the sake of analyses, a nondimensionalized form of the governing equations is provided. Later, linear stability analysis is conducted by using the D-subdivision scheme. In Section 4, the solutions of the nonlinear system are examined by using a continuation method. The implicit state-dependent delay is rewritten as an explicit function by using a Taylor expansion to facilitate the analysis. Hopf bifurcations of fixed points are determined and it is found that the nature of these bifurcations can be subcritical or supercritical depending on the parameter values. It is found that the state-dependent delay can have a destabilizing effect in certain cases. The axial damping ratio and torsion damping ratio are found to have a significant influence in determining the effect of the state-dependent delay on the system dynamics.

2   Modeling and nondimensionalization

In Figure 1(a), an illustrative model of a drill-string system is provided. The axial and torsion motions of interest are also shown. At the top end of the drill sting, a constant axial speed V_0 and a rotation speed Ω_0 are imposed on the system. The governing equations of motion take the form

$$
\begin{aligned}
M\ddot{Z}(t) + C_a\dot{Z}(t) + K_a(Z(t) - V_0 t) &= W_s - W_b(t) \\
I\ddot{\Phi}(t) + C_t\dot{\Phi}(t) + K_t(\Phi(t) - \Omega_0 t) &= -T_b(t)
\end{aligned}
\tag{1}
$$

Here, M and I are the respective translational and rotational inertias, K_a and K_t are the respective translational stiffness and torsion stiffness, and C_a and C_t represent the respective translational damping and torsion damping. Furthermore, W_s is the sum of the weight of both the drill pipe and drill collar. W_b and T_b respectively denote the weight and torque on the bit, and they are both determined by bit-rock interactions. Each of them can be decomposed in terms of cutting and friction components, as follows.

$$
\begin{aligned}
W_b(t) &= W_{bc}(t) + W_{bf}(t) \\
T_b(t) &= T_{bc}(t) + T_{bf}(t)
\end{aligned}
\tag{2}
$$

The subscripts bc denotes the cutting component of the drill bit and bf denotes the friction components on the drill bit, respectively. Following the earlier work of Detournay and Defourny[6], those components can be expressed as

$$
W_{bc}(t) = \epsilon a \zeta R(d(t)) H(\dot{\Phi}(t)) \qquad T_{bc}(t) = \frac{1}{2}\epsilon a^2 R(d(t)) H(\dot{\Phi}(t))
\tag{3}
$$

$$
W_{bf}(t) = \sigma a l H(d(t)) H(\dot{Z}(t)) \qquad T_{bf}(t) = \frac{1}{2}\mu\gamma a^2 \sigma l sgn(\dot{\Phi}) H(d(t)) H(\dot{Z}(t))
\tag{4}
$$

where the $R(.)$ function is the unit ramp function and $H(.)$ is the Heaviside step function. In Figure 1, two successive blades of a polycrystalline diamond compact drill bit are shown along with the delayed states. For an individual blade, the instantaneous depth of cut can be determined as

$$
d_n(t) = Z(t) - Z(t - \tau)
\tag{5}
$$

Assuming that the cutting action is uniform across the N blades, then, the cutting depth is

$$
d(t) = N d_n(t)
\tag{6}
$$

where the delay τ is given by

$$
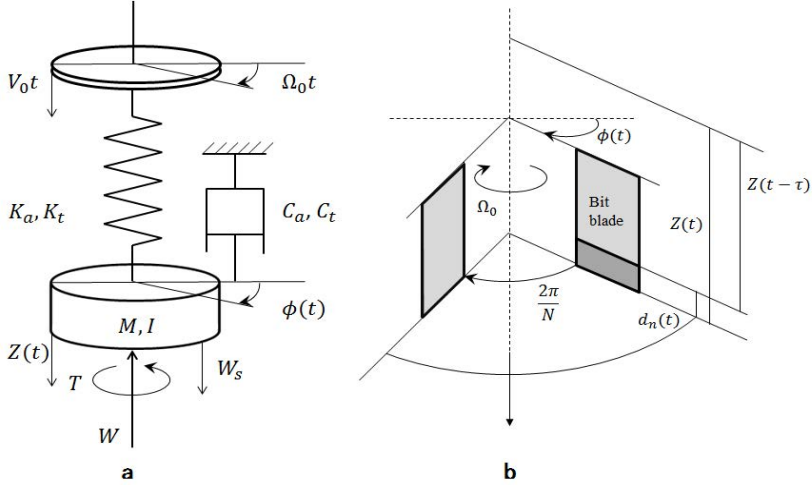\Phi(t) - \Phi(t - \tau) = \frac{2\pi}{N}
\tag{7}
$$

2

Figure 1: (a) Representative reduced-order model of drill-string system. (b) Two successive blades of a drill bit.

The state-dependent delay $\tau(\Phi(t))$ is the elapsed time for the drill bit to rotate over an angle of $\frac{2\pi}{N}$, and this delay depends only on the state Φ. Next, the equations of motion are cast into dimensionless form. Following earlier work [2], the characteristic time $t_* = \sqrt{I/K_t}$ and characteristic length $L_* = 2K_t/\epsilon a^2$ are introduced. Then, once can write the nondimensional variables as

$$z = \frac{Z - \bar{Z}}{L_*} \qquad \varphi = \Phi - \bar{\Phi} \qquad \hat{t} = t/t_* \qquad \hat{\tau} = \tau/t_* \tag{8}$$

Here, $\bar{Z}$, and $\bar{\Phi}$ correspond to the equilibrium solution of Eq.(1), which is a trivial solution in the absence of vibrations. The axial state z and angular state φ are functions of dimensionless time $\hat{t}$. With the nondimensional variables, the governing equations can be recast as

$$\begin{aligned}
\ddot{z}(\hat{t}) + 2\xi\eta\dot{z} + \eta^2 x(\hat{t}) &= -\psi\delta(\hat{t}) \\
\ddot{\varphi}(\hat{t}) + 2\kappa\dot{\varphi}(\hat{t}) + \varphi(\hat{t}) &= -\delta(\hat{t})
\end{aligned} \tag{9}$$

The dimensionless parameters are defined as

$$\xi = \frac{C_a}{2\sqrt{K_a M}} \qquad \kappa = \frac{C_t}{2\sqrt{K_t I}} \tag{10}$$

$$\psi = \frac{\epsilon a \zeta I}{K_t M} \qquad \eta^2 = \frac{K_a}{M} t_*^2 = \frac{K_a I}{K_t M}$$

Table 1: Parameters used for drilling operations (values adopted from references [1, 4])

Parameter	Symbol	Value	Unit
Mass	M	3.4×10^4	kg
Axial damping	C_a	1.56×10^4	N s/m
Axial stiffness	K_a	7.0×10^5	N/m
Moment of inertia	I	116	kg m^2
Torsion damping	C_t	32.9	N s m/rad
Torsion stiffness	K_t	938	N/m
Radius of drill bit	a	0.108	m
Wear flat length	l	0.0012	m
Intrinsic specific energy of rock	ϵ	$0 - 110$	MPa
Contact strength	σ	60	Mpa
Cutter face inclination	ζ	0.6	-
Friction coefficient	μ	0.6	-
Geometry parameter of drill bit	γ	1	-
Number of blades on drill bit	N	4	-

The parameters ξ and κ are the damping ratios associated with axial and torsional motions, respectively. η represent the ratio of axial natural frequency to torsional natural frequency. The quantity ψ is dependent upon the rock strength and drill-bit geometry.

δ is the dimensionless perturbation of cutting depth δ, and this can be written as

$$\delta(\hat{t}) = N[z(\hat{t}) - z(\hat{t} - \hat{\tau}) + (\hat{\tau} - \hat{\tau}_0)v_0] \tag{11}$$

where v_0 is the dimensionless penetration rate, ω_0 is the dimensionless angular speed, and $\hat{\tau}_0$ is the constant steady-state time delay. These quantities take the forms

$$\omega_0 = \Omega_0/t_* \qquad v_0 = \frac{V_0/L_*}{\Omega_0} = \frac{\epsilon a^2}{2K_t\Omega_0}V_0 \qquad \hat{\tau}_0 = \frac{2\pi}{N\omega_0} \tag{12}$$

The dimensionless state-dependent delay is given by

$$\hat{\tau} = \hat{\tau}_0 - \frac{1}{\omega_0}(\varphi(\hat{t}) - \varphi(\hat{t} - \hat{\tau})) \tag{13}$$

After substituting Eq.(11) and Eq.(13) into Eq.(9), the governing equations

4

can be rewritten as

$$\ddot{z}(\hat{t}) + 2\xi\eta\dot{z}(\hat{t}) + \eta^2 z(\hat{t}) = -N\psi(z(\hat{t}) - z(\hat{t} - \hat{\tau})) + N\psi v_0(\varphi(\hat{t}) - \varphi(\hat{t} - \hat{\tau}))$$

$$\ddot{\varphi}(\hat{t}) + 2\kappa\dot{\varphi}(\hat{t}) + \varphi(\hat{t}) = -N(z(\hat{t}) - z(\hat{t} - \hat{\tau})) + Nv_0(\varphi(\hat{t}) - \varphi(\hat{t} - \hat{\tau})) \quad (14)$$

3 Linear stability

According to the work of Hartung [7], a true linearization of the system with state-dependent delay is not possible due to the fact that the solution of the system is not differentiable with respect to state-dependent delay. Hence, one needs to find a constant delay model which has the same local stability properties as the original system. Making use of the method discussed by Insperger and Stepan [8],and letting $\hat{\tau} = \hat{\tau}_0$, the resulting linearized system is

$$\ddot{z}(\hat{t}) + 2\xi\eta\dot{z}(\hat{t}) + \eta^2 z(\hat{t}) = -N\psi(z(\hat{t}) - z(\hat{t} - \hat{\tau}_0)) + N\psi v_0(\varphi(\hat{t}) - \varphi(\hat{t} - \hat{\tau}_0))$$

$$\ddot{\varphi}(\hat{t}) + 2\kappa\dot{\varphi}(\hat{t}) + \varphi(\hat{t}) = -N(z(\hat{t}) - z(\hat{t} - \hat{\tau}_0)) + Nv_0(\varphi(\hat{t}) - \varphi(\hat{t} - \hat{\tau}_0)) \quad (15)$$

From these linearized equations, the characteristic equation is determined as

$$P_0(s) + P_1(s)(1 - e^{-\bar{\tau}s}) = 0 \quad (16)$$

where P_0 and P_1 are polynomials in the eigenvalue s. These polynomials can be determined as

$$P_0(s) = s^4 + (2\xi\eta + 2\kappa)s^3 + (\eta^2 + 4\kappa\xi\eta + 1)s^2 + (2\xi\eta + 2\kappa\eta^2)s + \eta^2$$

$$P_1(s) = (N\psi - Nv_0)s^2 + (2\kappa N\psi - 2\xi\eta Nv_0)s + (N\psi - N\eta^2 v_0) \quad (17)$$

Following the procedure of the D-subdivision method, the authors substitute $s = i\omega$ and $\bar{\tau} = 2\pi/\omega_0$ into Eqs.(17) and separate the real and imaginary parts. After a rather lengthy calculation, one obtains the stability crossing set in the ω_0-v_0 domain as

$$v_{0SDD} = \frac{1}{N[\alpha(\omega^2 - \eta^2) + 2\beta\xi\eta\omega]} \left[\frac{\alpha^2 + \beta^2}{2} + (\alpha(1 - \omega^2) + 2\beta\kappa\omega)N\psi \right]$$

$$\omega_{0_SDD} = \frac{2\pi\omega}{N(\Theta_1 + (2k-1)\pi)}, \qquad k = 1, 2, ..., \quad (18)$$

Here,

$$\alpha = Real(P_0) \qquad \beta = Imag(P_0) \qquad \Theta_1 = \angle \frac{-P_1}{P_0 + P_1} \quad (19)$$

 Results obtained on the basis of stability boundaries in the $\omega_0 - v_0$ parameter space is shown in Figure 2. From the plots, it is evident that the damping ratios play an important role in determining the stability boundaries. The results obtained agree well with the numerical findings reported in an earlier work by the authors' group [4].
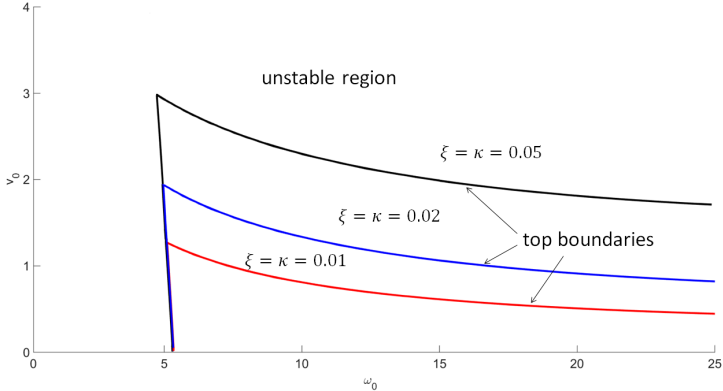
Figure 2: Stability charts in the plane of the drive speed ω_0 and the penetration speed v_0, for different values of ξ and κ.

4 Nonlinear analysis of the system with the state-dependent delay

In Eq.(14), the state-dependent delay term is the only source for nonlinearity of our nondimensionalized system and it is in term of implicit function. The software DDE-BIFTOOL [10] can be used to carry out continuation of solution branches of systems with delays. Here, this tool is used to study the bifurcations of solution of the nonlinear systems with constant delay and state-dependent delay. However, to use this tool, the state-dependent delay must be in an explicit form. To address this, the state-dependent delay in Eq.(13) is rewritten as a three level, nested constant delay in the form

$$\hat{\tau} = \hat{\tau}_0 - \frac{1}{\omega_0}(\varphi(\hat{t}) - \varphi(\hat{t} - (\hat{\tau}_0 - \frac{\varphi(\hat{t}) - \varphi(\hat{t} - \hat{\tau}_0)}{\omega_0}))) \tag{20}$$

By using a Taylor expansion and only keeping the first two orders, the explicit form of state dependent delay is determined as

$$\hat{\tau} = \hat{\tau}_0 - \frac{1}{\omega_0}(\varphi(\hat{t}) - \varphi(\hat{t} - \hat{\tau}_0)) - \frac{1}{\omega_0^2}(\varphi(\hat{t}) - \varphi(\hat{t} - \hat{\tau}_0))\dot{\varphi}(\hat{t} - \hat{\tau}_0) \tag{21}$$

After combining the nondimensionalized governing system Eqs. (14) together with the explicit state-dependent delay function Eq.(21) and using the DDE-BIFTOOL, the authors generate the bifurcation diagram with different dimensionless damping ratios as shown in Figure 3. The continuation of the periodic

orbits is stopped, when the state-dependent delay $\hat{\tau} < 0$. Along the y axis, the maximum value of the dimensionless φ of the orbit is shown.

Similarly to the turning case [9], when a subcritical Hof bifurcation of a fixed point occurs, an unstable limit cycle (periodic orbit) coexists with the stable equilibrium. When a supercritical Hopf bifurcation of a fixed point occurs, an stable limit cycle (periodic orbit) coexists with the unstable equilibrium. From the figures, it can be discerned that when the dimensionless axial and torsional damping ratios are small, branches of periodic motions bend to the left locally; this is a characteristic of a subcritical bifurcation. However, as the damping ratios are increased, the periodic solution branches start to bend to the right; this menas that the nature of the Hopf bifurcation has changed from subcritical to supercritical.

5   Concluding remarks

In this work, the effect of the state-dependent delay on drilling dynamics has been elucidated by considering a representative reduced-order model for coupled axial and torsion dynamics. The linear stability of the equilibrium solution of the system was analyzed by using the D-subdivision method, and the nonlinear stability analysis was conducted with the aid of a continuation scheme. From the results, it can be inferred that both the axial damping ratio and torsion damping ratio play a significant role in determining the linear stability of the equilibrium solution and the nature of the Hopf bifurcation of the equilibrium solution.

References

[1] Richard,T., Germay, C., and Detournay, E. (2007) A simplified model to explore the root cause of stickslip vibrations in drilling systems with drag bits. J. Sound Vib. 305(3),432-456.

[2] Besselink,B., van de Wouw, N., and Nijmeijer, H.(2011) A semi-analytical study of stick-slip oscillations in drilling systems. ASME J. Comput. Nonlinear Dyn. 6(2),p.021006.

[3] Liu X., Vlajic N., Long X., Meng G., and Balachandran B.(2014) State-dependent delay influenced drill-string oscillations and stability analysis ASME J. Vibration and Acoustics DOI: 10.11115/1.4027958.

[4] Liu X., Vlajic N., Long X., Meng G., and Balachandran B. (2014) Coupled axial-torsional dynamics in rotary drilling with state-dependent delay: stability and control J. Non-linear Dyn 78:1891-1906.
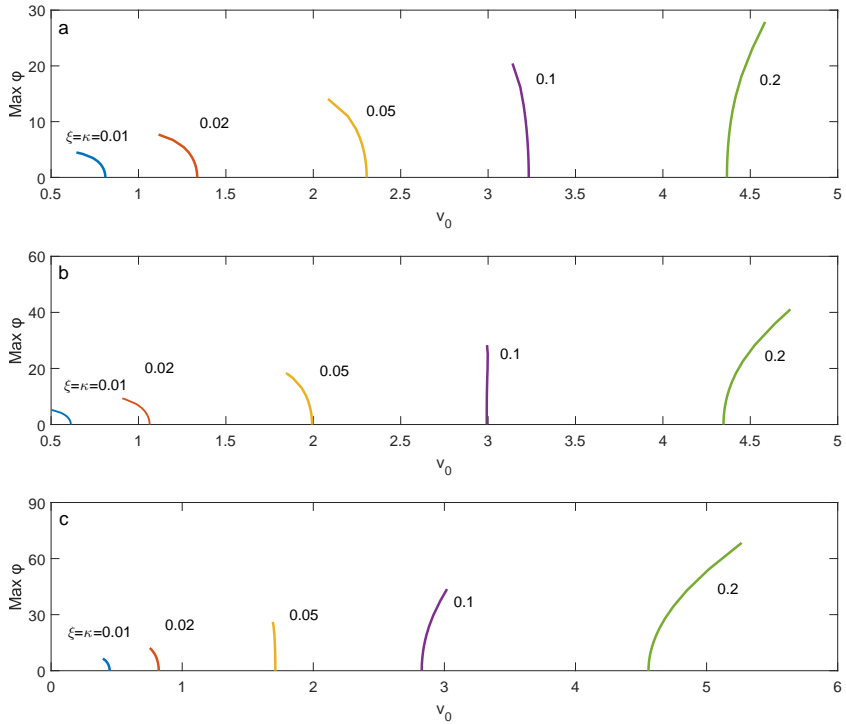
Figure 3: Stability charts in the plane of the drive speed ω_0 and the penetration speed v_0, for different values of the damping ratios ξ and κ: (a) $\omega_0 = 10$, (b) $\omega_0 = 15$, and (c) $\omega_0 = 25$.

[5] Zheng X. and Balachandran B. (2017) State-Dependent Delay and Drill-String Dynamics. Procedia IUTAM, Volume 22, 31-38.

[6] Detournay,E., and Defourny, P.(1992) A phenomenological model for the drilling action of drag bits. Int. J. Rock Mech. Min. Sci. Geomech. Abstr.,29(1):13-23.

[7] Hartung F. and Turi J. (2000) Linearized stability in functional-differential equations with stat-dependent delays. Proceeding of the conference Dynamical Systems and Differential Equations, added volume of Discrete and Continuous Dynamical Systems: 416-425.

[8] Insperger T., Stepan G., and Turi J.(2007) State-dependent delay in regenerative turning processes, Nonlinear Dyn. 47(1-3): 275-283.

[9] Insperger T., Barton D. A. W., and Stepan G. (2007) Criticality of Hopf bifurcation in state-dependent delay model of turning processes Int. J. Non-Linear Mechanics 43: 140-149.

[10] K. Engelborghs, T. Luzyanina, G. Samaey, DDE-BIFTOOL v.2.00: a Matlab package for bifurcation analysis of delay differential equations, Technical Report TW 330, Department of Computer Science, K.U.Leuven, Leuven, Belgium, 2001.

Roman J. Shor[1], Ulf Jakob F. Aarsnes[2] and Florent di Meglio[3]

[1]University of Calgary, Calgary, Canada
[2]International Research Institute of Stavanger (IRIS), Oslo, Norway
[3]Mines ParisTech, Paris, France

1 Introduction

Exploration and production of oil and gas in the deep subsurface, where hydrocarbon reservoirs are found at depths between 2,000 and 20,000 feet, requires that a narrow borehole, between 4 and 24 inches in diameter, be drilled using a slender drill string through a varied downhole environment and along an often snaking wellpath. Drill string vibrations, and their negative consequences on ROP and equipment, is a well known phenomenon when drilling for hydrocarbons. In particular, the torsional oscillations known as stick slip, which are considered to be the most destructive vibrations, are to be avoided.

Significant literature exists which seeks to explain the incidence of stick slip through various implementations of bit-rock interaction and various complexities of drill string dynamic models. The simplest models impose bit-rock interaction as a discontinuous frictional force at the bit and abstract the drill string as a lumped mass, representing the bottom hole assembly (BHA) inertia, and a torsional spring, representing the drill-string stiffness [5, 6]. These models may be confounded by introducing higher complexity dynamics at the bit-rock interaction or through higher order models along the drill-string [12, 13], but still assume that stick slip is incided due to the non-linearity of the frictional force at the bit. pAll these models have used to demonstrate the occurrence of the limit cycle which exhibits itself as stick-slip and may be used to various types of stick-slip mitigation controllers, including simple tuned PID controllers [11, 15], impedance matching controllers [7], H-infinity controllers [16], sliding mode controllers [14], and others.

2 Model

We use a distributed model, similar to [4, 3, 8] and described in detail in [2], where we consider only the torsional dynamics of the drill string. For angular motion, angular velocity and torque are denoted as as $\omega(t, x), \tau(t, x)$, respectively, with $(t, x) \in [0, \infty) \times [0, L]$. See Fig. 1 for a schematic indicating locations. For an infinitesimal element dx, the torque is found as the shear strain, or twist per unit length. Letting ϕ denote the angular displacement in the string s.t. $\frac{\partial \phi(t,x)}{\partial t} = \omega(t, x)$, we have $\tau(t, x) = JG\big(\phi(t, x) - \phi(t, x+dx)\big)/dx$, where J is the polar moment for inertia and G is the shear modulus. Hence the equations for the angular motion are given by

$$\frac{\partial \tau(t, x)}{\partial t} + JG\frac{\partial \omega(t, x)}{\partial x} = 0 \tag{1}$$

$$J\rho\frac{\partial \omega(t, x)}{\partial t} + \frac{\partial \tau(t, x)}{\partial x} = S(\omega, x), \tag{2}$$

where the source term S is modeled as

$$S(\omega, x) = -k_t \rho J \omega(t, x) - \mathcal{F}(\omega, x), \tag{3}$$

where k_t is a damping constant representing the viscous shear stresses and $\mathcal{F}(\omega)$ is a differential inclusion, to be described, representing the Coulomb friction between the drill string and the borehole. The viscous shear stress coefficient k_t represnts the combined damping effects of the viscous shear of the drilling mud and the rolling contact between drill string and the cuttings bed.

The lowermost section of the drill string is typically made up of drill collars which may have a great impact on the drill string dynamic due to their added inertia. In particular, the transition from the pipes to collars in the drill string will cause reflections in the traveling waves due to the change in characteristic line impedance [4]. We split the drill string into a pipe section with polar moment of inertia and lengths J_p, L_p and a collar section with the same parameters given as J_c, L_c.

2.1 Coulomb friction as an inclusion

The Coulomb friction is modeled as an inclusion

$$\begin{cases} \mathcal{F}(\omega, x) = F_d(x), & \omega > \omega_c, \\ \mathcal{F}(\omega, x) \in [-F_c(x), F_c(x)], & |\omega| < \omega_c, \\ \mathcal{F}(\omega, x) = -F_d(x), & \omega < -\omega_c, \end{cases} \tag{4}$$
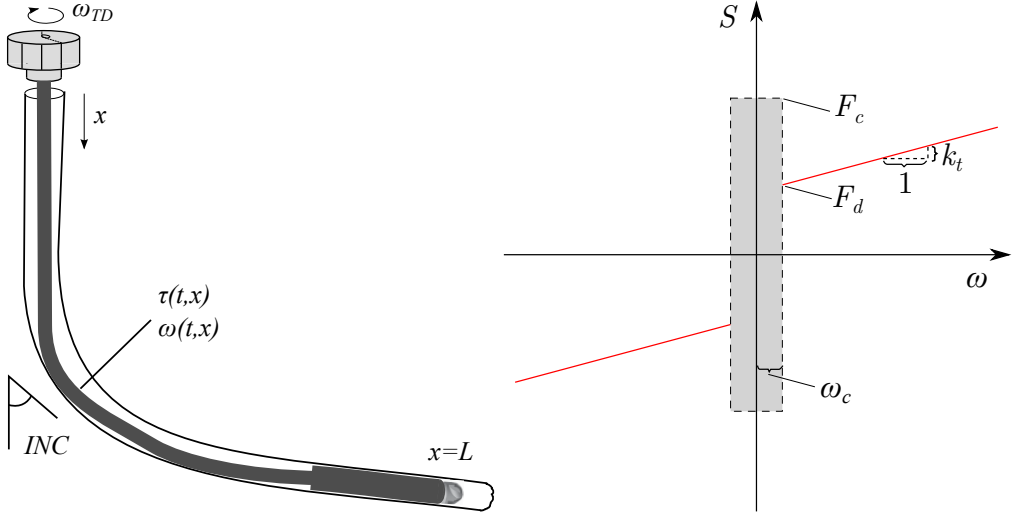
Figure 1: Schematic indicating the distributed drill string lying in deviate bore-hole (left). Schematic illustrating the four parameters determining the friction: the coulomb friction parameters ω_c, F_c, F_d and the viscous friction coefficient k_t, with the shaded region indicating the region of static torque, and the red curve the dynamic torque (right).

where ω_c is the threshold on the angular velocity where the Coulomb friction transitions from static to dynamic, F_d is the dynamic Coulomb torque, F_c is the static Coulomb torque, and $\mathcal{F}(\omega) \in [-F_c, F_c]$ denotes the inclusion where

$$\mathcal{F}(\omega, x) = -\frac{\partial \tau(t, x)}{\partial x} - k_t \rho J \omega(t, x) \in [-F_c(x), F_c(x)], \tag{5}$$

and take the boundary values $\pm F_c(x)$ if this relation does not hold. We define the non-dimensional coefficient $f_{rat} = F_c/F_d$ to help characterize the magnitude of the oscillations. The shape of the friction source term is illustrated in Fig. 1.

3 Model comparison with field data

To validate the modeling approach taken in the present work, a simulation study was undertaken to compare the behavior of the model to that of recorded field data. A field comparison is presented which exhibits inerita dominated oscillations, as categorized in [2]. Field data for a deviated well, the survey of which is shown in Figure 2, is considered. Rotational data – rotary rpm and torque – is recorded at 100 Hz and includes both setpoints and realized values. The
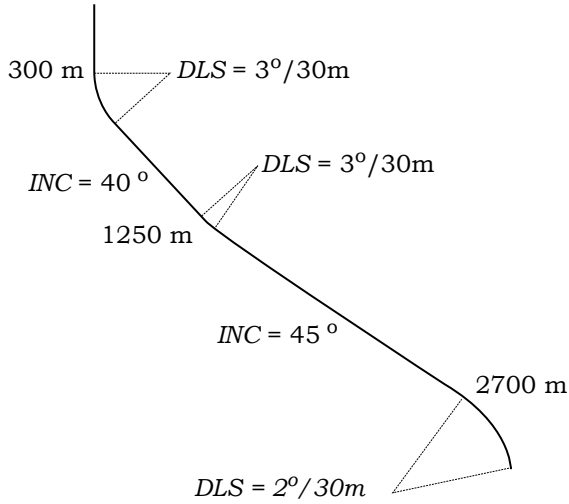
Figure 2: Wellbore survey of the field well

drill-string starts at rest with zero torque at the surface. However, the stored torsional energy within the drill-string is not known. The drill-string design is a
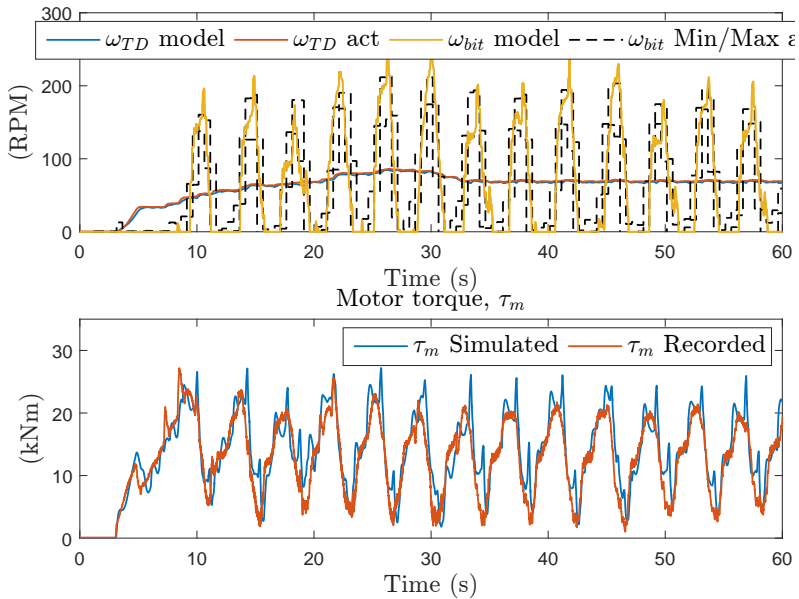

Figure 3: Recorded and simulated drill-string response at a bit depth of 1,733 m, using fitting parameters: $\mu = 0.34, f_{rat} = 0.55, \omega_c = 19$ (RPM).
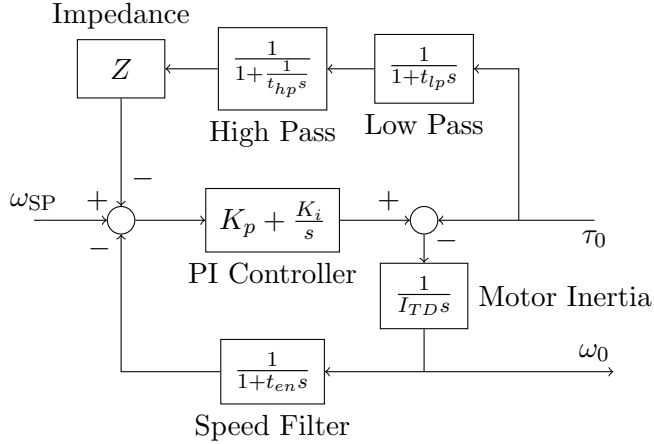
14

Figure 4: Control diagram for a ZTorque system with direct pipe torque measurement. For ZTorque $Z = 1/\zeta_p$ is used. If $Z = 0$, the control diagram is equivalent to a SoftTorque or stiff speed controller system.

simple directional assembly which is simplified to a 230 meter $5\frac{3}{4}$" OD BHA and monodiameter drillpipe to the surface. Downhole rpm and vibration data was collected for drilling performance improvement and control system verification and included continuous low frequency (0.5Hz) data as well as occasional burst sequences of high frequency data (125 Hz).

Recorded field data and a model fit for 1,733 m depth is shown in Figure 3. The top plot shows the surface (in red) and downhole (dashed) recorded data as well as the modeled data (in blue and yellow, respectively). The bottom plot shows surface torque, with recorded data in red and simulated data in blue.

4 Stick-slip Mitigation Controllers

A majority of drilling rigs in the field utilize AC electric top drives controlled using a variety of variable frequency drives – or inverters – which are capable of highly accurate, and often high frequency (> 20 Hz), rotary speed control. A majority of these controllers are simple stiff PI controllers, but two types of stick-slip mitigation controllers are widely deployed – the older SoftTorque / SoftSpeed systems and the newer ZTorque systems.

The behavior of a control system may evaluated through the use of a topside reflection coefficient – a reflection of '1' indicates all energy is reflected back downhole, while a reflection of '0' means all energy is absorbed by the topdrive. Assuming for the moment a constant set-point, and defining the controller trans-

fer function $C(s) \equiv \frac{\tau_m}{\omega_0}$ we obtain the relation:

$$\frac{\tau_0(s)}{\omega_0(s)} = C(s) + I_{TD}s \equiv \bar{C}(s), \tag{6}$$

while the topside reflection coefficient is given as [11]

$$R(\omega) = \left| \frac{\bar{C}(s) - \zeta_p}{\bar{C}(s) + \zeta_p} \right|_{s=j\omega}. \tag{7}$$

4.1 Stiff controller

The industry standard controller that is most often used is a high gain PI control to ensure rapid tracking of the top drive set-point. For this study, we use the gains

$$K_p = 100\zeta_p, \qquad K_i = 5I_{TD}. \tag{8}$$

which is similar to gains typically used in the field.

4.2 SoftTorque

The current industry standard in handling torsional vibrations are the two products NOV's SoftSpeed [11, 9] and Shell's SoftTorque [7, 15]. The essential approach of all these solutions is to reduce the reflection coefficient at the top drive in a certain key frequency range [10].

The approach of SoftSpeed [11] is to set the proportional action to

$$K_p = 4\zeta_p, \tag{9}$$

and then tune the integral gain according to

$$K_i = (2\pi f_c)^2 I_{TD}^2, \tag{10}$$

where f_c is the frequency (in Hertz) where the minimum of $R(\omega)$ is achieved. Since the transfer funciton of an ideal PID controller writes $C(s) = K_p + \frac{K_i}{s} + K_d s$, the minimum of the reflection coefficient is obtained at

$$\underset{\omega}{\mathrm{argmin}}\, R(\omega) = \sqrt{\frac{K_i}{I_{TD} + K_d}} \equiv f_c 2\pi. \tag{11}$$
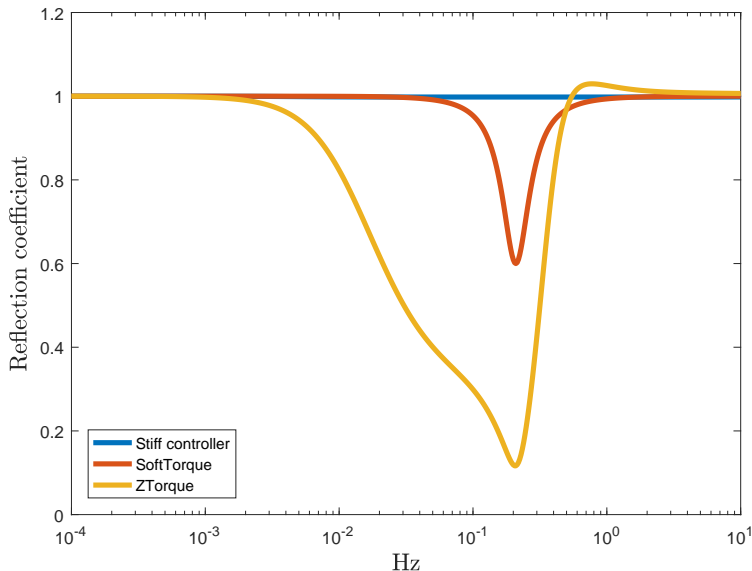
16

Figure 5: Topside reflection coefficient of the three considered controllers.

4.3 ZTorque

A newer embodiment of stick-slip mitigation control developed by Shell, *ZTorque*, seeks to minimize the reflection coefficient of the top drive for a wider range of frequencies by measuring the torque from between the drill string and top-drive τ_0, and using this in the feedback controller to "artificially" have the top-drive match the impedance of the drill-pipe ζ_p. The drill pipe impedance is given as $\zeta_p = J_p\sqrt{G_p\rho}$ where ζ_p is the characteristic line impedance of the drill string.

For a given pipe torque, the instantenous top drive rotary velocity necessary to match the pipe impedance is given by:

$$\omega_0(t) = \frac{1}{\zeta_p} \cdot \tau_0(t) \tag{12}$$

To ensure set point tracking, the control system uses a bandpass filter on the impedance matching rotary velocity – to exclude high frequency noise and low frequency set point changes – by combining a high-pass and low pass filter. Therefore, the PI controller acts on a combination of the tracking error $\omega_{\mathrm{SP}-\omega_0}$, and the band-pass filtered measured pipe torque $Z\frac{1}{s+\frac{1}{t_{hp}s}}\frac{1}{s+t_{lp}s}\tau_0$, i.e. the input

17

to the PI controller is

$$e_{PI} = \omega_{\mathrm{SP}} - \omega_0 - Z \frac{s}{(s + \frac{1}{t_{hp}})(1 + t_{lp}s)} \tau_0 \qquad (13)$$

where t_{hp}, t_{lp} are the high pass, low pass filter time constants. Note that the ω_0 measurement passes through an encoder, illustrated in Fig. 4 as a low-pass filter with time constant t_{en}. Typically, t_{lp} and t_{en} are around 1 to 10 milliseconds and t_{hp} is around 2 to 10 seconds but must be greater than the period of the first mode of stick-slip. The implementation studied in this talk assumes the presence of a torque sensor between the top drive and drillstring which is capable of real-time measurement of pipe torque, τ_0.

Topside reflection coefficient of the three considered controllers is shown in Fig. 5. The SoftTorque controller uses $K_p = 4\zeta_p, f_c = 0.2(\mathrm{Hz})$ and the ZTorque controller a 1 ms speed and low pass filters and a 10 second high pass filter.

5   Simulation study

We consider a rotation startup such as is required after each pipe connection procedure while drilling a well. In this scenario the stationary drill string is initially kept in place by the Coulomb friction until enough torque is built up to overcome it. At which point, pipe-rotation is initiated and the Coulomb friction is reduced as it changes from static to dynamic. The resulting release of the stored energy potentially pushes the drill string into a destructive stick slip limit cycle. We refer to [2] for a more detailed description of this phenomena, where it is shown that the simulation model used in the present talk is capable of effectively replicating this type of stick-slip phenomenon.

Figure 6 depicts time series of the bottom rotational velocity and topside torque for two sets of friction parameters μ and f_{rat}. It is clear from these simulations that ZTorque yields a much slower controller, but one that effectively avoids reflections in the relevant frequency range, thus mitigating the tendency of stick slip. The length of time necessary to reach the setpoint rotation speed is directly related to the time costant of the high pass filter in the ZTorque system. It is also clear that the severity of the stick slip, and the tendency of such oscillation to be initiated, is highly dependent on the friction parameters μ, f_{rat}. A thorough treatise of the topic is presented in [1].

6   Sensitivity to filtering and latency

Latency and filtering in rig systems may be included directly in the control system model presented above, and by evaluating the topside reflectivity as a
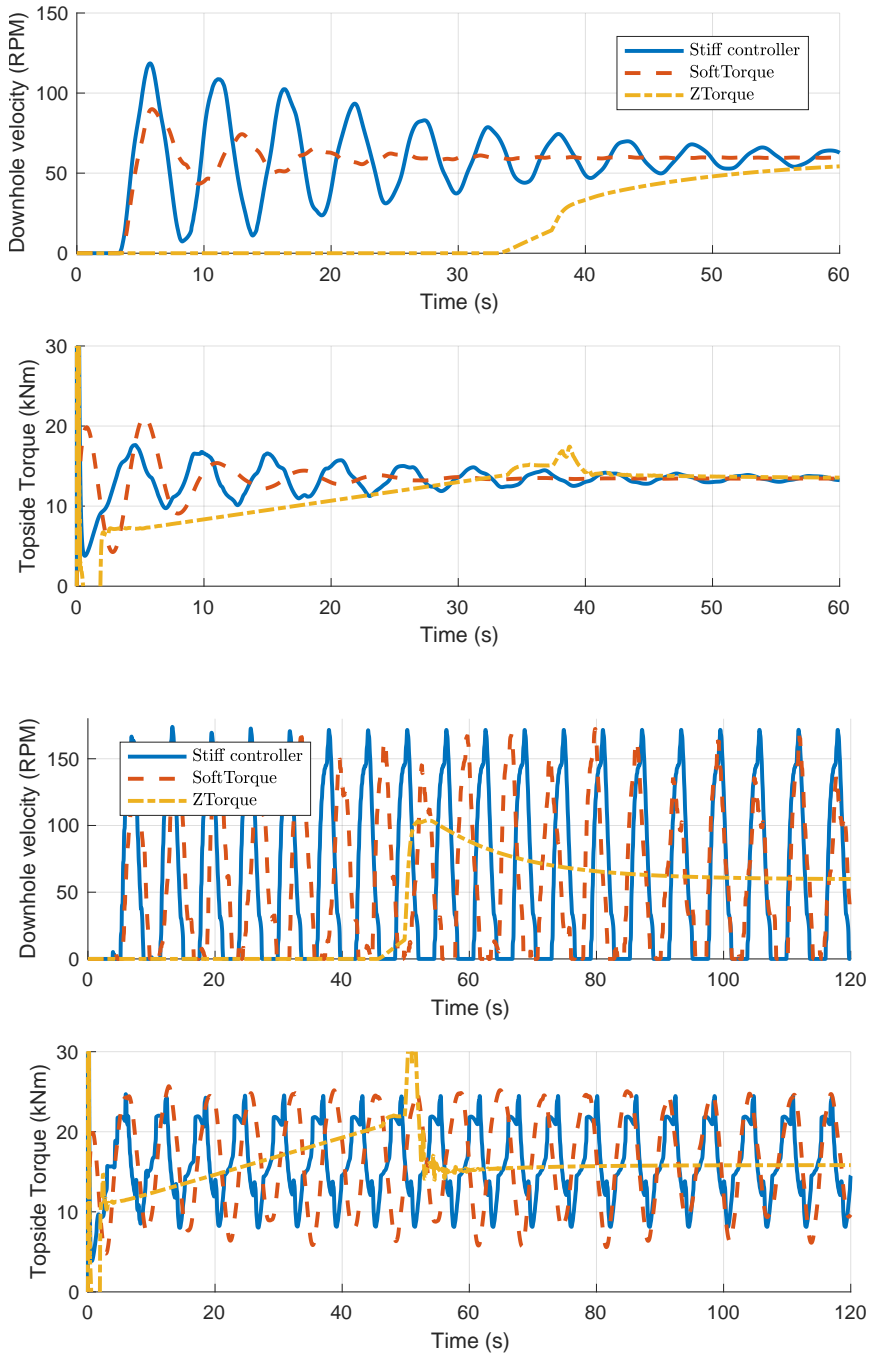
Figure 6: Bottom velocity (top) and topside torque (bottom) as a function of time, for $\mu = 0.2$ and $f_{rat} = 0.75$ (top) and $\mu = 0.3$ and $f_{rat} = 0.85$ (bottom), for each of the three controllers.

function of frequency, their effects on performance may be quantified. During this talk, a series of examples will be presented which will include the effects of top drives with large inertias, highly filtered torque or speed sensors and delays in inverter - control system communication. Every increase in filtering or latency leads to a decrease in system performance, but this performance degradation may still yield an effective system in certain scenarios.

References

[1] Ulf Jakob F Aarsnes, Florent Meglio, and Roman J Shor. Benchmarking of Industrial Stick-Slip Mitigation Controllers. In *IFAC Workshop on Automatic Control in Offshore Oil and Gas Production*, 2018.

[2] Ulf Jakob F. Aarsnes and Roman J Shor. Torsional vibrations with bit off bottom: Modeling, characterization and field data validation. *Journal of Petroleum Science and Engineering*, 163:712–721, apr 2018.

[3] Ulf Jakob F. Aarsnes and Nathan van de Wouw. Dynamics of a distributed drill string system: Characteristic parameters and stability maps. *Journal of Sound and Vibration*, 417:376–412, mar 2018.

[4] Ulf Jakob Flø Aarsnes and Ole Morten Aamo. Linear stability analysis of self-excited vibrations in drilling using an infinite dimensional model. *Journal of Sound and Vibration*, 360:239–259, jan 2016.

[5] J J Bailey and I. Finnie. An Analytical Study of Drill-String Vibration. *Transactions of the American Society of Mechanical Engineers*, (May 1960):122–127, 1960.

[6] Dmitriy Dashevskiy, Jens Rudat, and Linus Pohle. Model-Based Stability Analysis of Torsional Drillstring Oscillations. In *Proceedings of 2011 IEEE International Conferencce on Control Applications*, Denver, CO, 2011.

[7] Sicco Dwars. Recent Advances in Soft Torque Rotary Systems. In *Proceedings of 2015 SPE/IADC Drilling Conference*, number March, pages 17–19, London, United Kingdom, 2015.

[8] Christophe Germay, Vincent Denoël, and Emmanuel Detournay. Multiple mode analysis of the self-excited vibrations of rotary drilling systems. *Journal of Sound and Vibration*, 325(1-2):362–381, aug 2009.

[9] G.W. Halsey, A Kyllingstad, and A Kylling. Torque Feedback Used to Cure Slip-Stick Motion. In *SPE Annual Technical Conference and Exhibition*, pages 277–282. Society of Petroleum Engineers, apr 1988.

[10] Aage Kyllingstad. A Comparison of Stick-Slip Mitigation Tools. In *SPE/IADC Drilling Conference and Exhibition*, number March, pages 14–16. Society of Petroleum Engineers, mar 2017.

[11] Åge Kyllingstad and Pål Jacob Nessjøen. A New Stick-Slip Prevention System. In *Proceedings of SPE/IADC Drilling Conference and Exhibition*, number March, pages 17–19, 2009.

[12] R. I. Leine, D. H. van Campen, and W. J. G. Keultjes. Stick-slip Whirl Interaction in Drillstring Dynamics. *Journal of Vibration and Acoustics*, 124(2):209, 2002.

[13] K. Nandakumar and Marian Wiercigroch. Stability analysis of a state dependent delayed, coupled two DOF model of drill-string vibration. *Journal of Sound and Vibration*, 332(10):2575–2592, 2013.

[14] Eva M. Navarro-Lopez, Domingo Cort, and Domingo Cortes. Sliding-mode control of a multi-DOF oilwell drillstring with stick-slip oscillations. In *Proceedings of the 2007 American Control Conference*, pages 3837–3842, New York City, jul 2007. IEEE.

[15] D. John Runia, Sicco Dwars, and Ivo Petrus Jozef Maria Stulemeijer. A brief history of the Shell "Soft Torque Rotary System" and some recent case studies. In *SPE/IADC Drilling Conference*, pages 69–76. Society of Petroleum Engineers, mar 2013.

[16] Muhittin Yilmaz, Salman Mujeeb, and Naren Reddy Dhansri. A H-infinity control approach for oil drilling processes. *Procedia Computer Science*, 20:134–139, 2013.

Florent Di Meglio[1], Ulf Jakob Aarsnes[2], Roman Shor[3]

[1]Centre Automatique et Systèmes, Mines ParisTech, Paris, France
[2]International Research Institute of Stavanger (IRIS), Oslo, Norway
[3]University of Calgary, Calgary, Canada

1   Introduction

The drilling process involves transport phenomena: mechanical deformation waves, pressure waves propagating into the drilling fluid, or simply the transport of mud, cuttings, and oil and gas in UnderBalanced Operations (UBO). These dynamics are often coupled and take a growing importance when the length of the well increases.

From a systems and control perspective, the industrial needs related to these phenomena span the whole field: set point tracking and disturbance rejection for pressure control in Managed Pressure Drilling (MPD), disturbance estimation for kick management, state estimation in UBO to monitor the amount of gas in the well, parameter estimation to perform reservoir characterization, or stabilization for severe slugging and mechanical vibrations. All of these problems have in common their distributed nature and, most importantly, high uncertainty.

Although the distributed nature of the transport phenomena is not necessary the bottleneck for all of these questions, it appears that some cases require the associated delays and wave propagation to be taken into account. We review here advances in boundary control and estimation of hyperbolic Partial Differential Equations that could bring solutions to some of these issues. We believe that the methods developed the past few years have the potential to be successfully applied to problems in drilling. Towards this end, we illustrate an application to friction estimation during stick-slip oscillations.

2   Torsional vibrations dynamics

To motivate the theoretical developments and illustrate their potential, we describe here a control problem representative of the class we tackle. Consider the drill-string depicted on Figure 1. It undergoes lateral, torsional and axial vibrations that propagate as
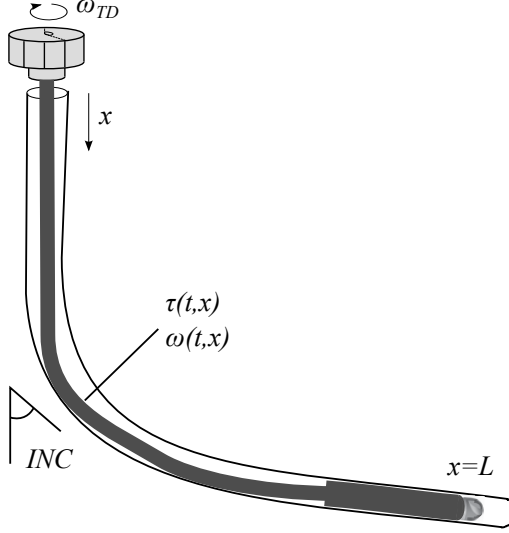
Figure 1: Schematic view of a drillpipe.

waves along its whole length. The causes for these detrimental oscillatory phenomena are many, generally associated with side forces [1] or cutting effects [12]. Importantly, the distributed nature of the wave propagation can play a predominant role, as illustrated in [4]. In [1], a model describing torsional dynamics is compared with field data, showing excellent accuracy. This result comes at the price of a careful tuning of the model parameters. More precisely, the model takes the form of a 1-D wave equation along the linear spatial dimension x, where the source term is due to frictional contact with the borehole and is modeled as

$$S(\omega, x) = -k_t \rho J \omega(t, x) - \mathscr{F}(\omega, x), \tag{1}$$

where k_t is a damping constant representing the viscous shear stresses between the pipe and drilling mud, $\omega(t, x)$ is the angular velocity at time t and position x, ρ is the pipe density and J its polar moment of inertia. The term $\mathscr{F}(\omega)$ is a differential inclusion, to be described, representing the Coulomb friction between the drill string and the borehole,

$$\begin{cases} \mathscr{F}(\omega, x) = F_d(x), & \omega > \omega_c, \\ \mathscr{F}(\omega, x) \in [-F_c(x), F_c(x)], & |\omega| < \omega_c, , \\ \mathscr{F}(\omega, x) = -F_d(x), & \omega < \omega_c, \end{cases} \tag{2}$$

where ω_c is the threshold on the angular velocity where the Coulomb friction transitions from static to dynamic, F_d is the dynamics Coulomb torque, and $\mathscr{F}(\omega) \in [-F_c, F_c]$

denotes the inclusion where

$$\mathscr{F}(\omega, x) = -\frac{\partial \tau(t,x)}{\partial x} - k_t \rho J \omega(t,x) \in [-F_c(x), F_c(x)], \tag{3}$$

and take the boundary values $\pm F_c(x)$ if this relation does not hold.

There is a large uncertainty in the distributed Coulomb friction terms $F_c(x)$, $F_d(x)$. In the next section, we design observers for hyperbolic PDEs in view of estimating these on-line from topside measurements only.

3   Control design for Hyperbolic PDEs: backstepping design

Backstepping is a control and observer design method first introduced for boundary control and observer design for PDEs in [13] and described in details in [8]. It relies on a change of variables such that control (resp. observer) design is "simple" in the new system of coordinates. We give here an example corresponding to the boundary control of two coupled transport equations which model, e.g., channel flow [3] or single-phase liquid flow, e.g. the annulus in Managed Pressure Drilling (MPD) [7]. Consider the following system of PDEs

$$\begin{pmatrix} u_t(t,x) \\ v_t(t,x) \end{pmatrix} + \begin{pmatrix} \lambda(x) & 0 \\ 0 & -\mu(x) \end{pmatrix} \begin{pmatrix} u_x(t,x) \\ v_x(t,x) \end{pmatrix} = \Sigma(x) \begin{pmatrix} u(t,x) \\ v(t,x) \end{pmatrix} \tag{4}$$

with the following boundary conditions

$$u(t,0) = d_0 v(t,0), \qquad\qquad u(t,1) = d_1 v(t,1) + U(t) \tag{5}$$

The variables u and v represent quantities (e.g. pressure waves) being transported along the spatial domain $x \in [0,1]$. The quantity u travels left to right while v travels in the opposite direction, i.e. we have $\lambda(x), \mu(x) > 0$. At the boundaries of the spatial domain, the waves are reflected with coefficients d_0 and d_1, with $|d_0 d_1| < 1$[1]. Inside of the domain, the two states are coupled through the matrix $\Sigma(x)$ typically representing friction and gravity effects. These coupling terms are responsible for poor transient performance and sometimes instability. Note that these equations usually stem from linearizing conservation laws around an equilibrium profile. Consider now the following change of coordinates

$$\begin{pmatrix} \alpha(t,x) \\ \beta(t,x) \end{pmatrix} = \begin{pmatrix} u(t,x) \\ v(t,x) \end{pmatrix} + \int_0^x K(x,y) \begin{pmatrix} u(t,y) \\ v(t,y) \end{pmatrix} dy \tag{6}$$

---

[1]This is a necessary assumption for the system to be robustly stabilizable [10].

Provided the kernel $K(x,y)$ is appropriately chosen, as described in [5], the equations satisfied by the new variables α and β read

$$\begin{pmatrix} \alpha_t(t,x) \\ \beta_t(t,x) \end{pmatrix} + \begin{pmatrix} \lambda(x) & 0 \\ 0 & -\mu(x) \end{pmatrix} \begin{pmatrix} \alpha_x(t,x) \\ \beta_x(t,x) \end{pmatrix} = 0 \qquad (7)$$

with the following boudary conditions

$$\alpha(t,0) = d_0\beta(t,0), \qquad \beta(t,1) = d_1\alpha(t,1) + U(t) + \int_0^x L(x,y) \begin{pmatrix} \alpha(t,y) \\ \beta(t,y) \end{pmatrix} dy \qquad (8)$$

for a certain known kernel $L(x,y)$. Notice that the coupling terms have been moved from the right-hand-side of the PDE to the controlled boundary of the domain. This suggests the following control law

$$U(t) = -k\alpha(t,1) - \int_0^x L(x,y) \begin{pmatrix} \alpha(t,y) \\ \beta(t,y) \end{pmatrix} dy \qquad (9)$$

where k is a design parameter used to trade-off performance versus robustness. Controller (9) ensures convergence of the solutions of (7)–(8) and, equivalently of (5)–(**??**) with a decay rate $\frac{1}{d_1-k}$. Imposing $k = d_1$ leads to finite-time convergence to zero in theory, but with vanishing robustness margins, as detailed in [10, 6, 2]. Transformation (6) serves as the basis for many extensions. In particular, in [5], a Luenberger observer is designed, relying on boundary measurements. In [11], a slightly more general state-feedback controller is obtained through a Port-Hamiltonian approach.

In [9], an integrator is added to (9) to reject constant disturbances, along with a boundary observer design with added design parameters. This result in an implementable output-feedback control law with three degrees of freedom that have an intuitive impact on set point tracking performance, robustness to noise and uncertainty and stability. In the next section, we show how these results can be extended to the more industry-relevant model described in Section 1.

4   Application to friction estimation

4.1   State and parameter observer design

To estimate unmeasured states and uncertain friction terms, we consider the following observer, based on an approximation of the model of [1] plus linear output error injec-

tion terms

$$\dot{\hat{\omega}}_0 = -a_0\hat{\omega}_0 + b_0\hat{v}(0,t) + B_U U(t) - p_0(\hat{\omega}_0 - y(t)) \tag{10}$$

$$\hat{u}(0,t) = c_0\hat{\omega}_0(t) + d_0\hat{v}(0,t) - P_0(\hat{\omega}_0 - y(t)) \tag{11}$$

$$\hat{u}_t(x,t) = -\lambda(x)\hat{u}_x(x,t) + \sigma^{++}(x)\hat{u}(x,t) + \sigma^{+-}(x)\hat{v}(x,t) - p_u(\hat{\omega}_0 - y(t)) \tag{12}$$

$$\hat{v}_t(x,t) = \mu(x)v_x(x,t) + \sigma^{-+}(x)\hat{u}(x,t) + \sigma^{--}(x)\hat{v}(x,t) - p_v(\hat{\omega}_0 - y(t)) \tag{13}$$

$$\hat{v}(1,t) = c_1\hat{\omega}_1(t) + d_1\hat{u}(1,t) - P_1(\hat{\omega}_0 - y(t)) \tag{14}$$

$$\dot{\hat{\omega}}_1 = -a_1\hat{\omega}_1 + b_1\hat{u}(1,t) + \hat{d}(t) - p_1(\hat{\omega}_0 - y(t)) \tag{15}$$

with

$$\begin{cases} d(\omega) = \hat{d}_d, & \hat{\omega}_1 > \omega_c, \\ d(\omega) \in [-\hat{d}_c, \hat{d}_c], & |\hat{\omega}_1| < \omega_c, \\ d(\omega) = -\hat{d}_d, & \hat{\omega}_1 < -\omega_c. \end{cases} \tag{16}$$

and where $\hat{u}$, $\hat{v}$ are defined as

$$u = \hat{\omega} + \frac{c_t}{JG}\hat{\tau}, \quad \hat{v} = \hat{\omega} - \frac{c_t}{JG}\hat{\tau}, \tag{17}$$

where $c_t = \sqrt{\frac{\rho}{J}}$ is the velocity of the torsional wave. This model is obtained by writing the equations in Riemann coordinates and lumping the Bottom Hole Assembly (BHA) into a single inertial element of rotational velocity ω_1. Moreover, we have lumped the inclusion representing the Coloumb friction at the ODE giving the downhole boundary condition. This approximation is typically amenable given either of the following two assumptions:

- Stabilizers located at the BHA ensures that a significant part of the total torque on the drill-string from side forces is acting on the BHA.

- The inertia of the BHA is sufficiently large so as to ensure that the torque from the BHA is large compared to that of the distributed side forces on the pipe. This is a qualitative observation seen from simulations.

However, if both these points do not hold, the approximation could cause the approach described in this paper to fail. The parameters $\hat{d}_d$ and $\hat{d}_c$ are chosen to satisfy the following update laws

$$\begin{pmatrix} \dot{\hat{d}}_d(t) \\ \dot{\hat{d}}_c(t) \end{pmatrix} = \begin{cases} \begin{pmatrix} k_1(\omega_0 - y(t)) \\ k_2(\omega_0 - y(t)) \end{pmatrix} & |\hat{\omega}_1| > \omega_c \\ \begin{pmatrix} k_1(\omega_0 - y(t)) \\ -k_2(\omega_0 - y(t)) \end{pmatrix}, & |\hat{\omega}_1| < \omega_c, \end{cases} \tag{18}$$

with $k_1, k_2 > 0$. Using a transformation similar to (6), one can find values of the observer gains and update gains such that when the observer velocity is non-zero, i.e. the observer state is in slip mode (rather than sticking), then (10)–(15),(18) converges to the true state. Although no proof of convergence is available for the full nonlinear observer, this approach yields promising results when applied to field data, as described in Section 3.2.

4.2 Field data validation

We have validated the approach by applying it to a data set corresponding to a 1733 meter-long well with an inclination pattern similar to the one schematically depicted on Figure 1. Since no bottom velocity measurement is available for this dataset, we evaluate the performance of the observer using the following two metrics

- we use, as the plant, the simulation model of [1]. The result of this comparison is depicted on Figure 2: the BHA velocity is accurately estimated and the friction parameter estimates converge to constant values.

- we use field data and vary the initial condition of the friction parameter estimates. These results are depicted on Figure 3. One can readily check that the estimates converge to roughly the same value, regardless of the initial condition, suggesting some form of robustness of the proposed approach.

References

[1] Ulf Jakob F. Aarsnes and Roman J Shor. Torsional vibrations with bit off bottom: Modeling, characterization and field data validation. *Journal of Petroleum Science and Engineering*, 163:712–721, apr 2018.

[2] Jean Auriol and Florent Di Meglio. Minimum time control of heterodirectional linear coupled hyperbolic pdes. *Automatica*, 71:300–307, 2016.

[3] Georges Bastin and Jean-Michel Coron. On boundary feedback stabilization of non-uniform linear 2×2 hyperbolic systems over a bounded interval. *Systems & Control Letters*, 60(11):900–906, 2011.

[4] Eric Cayeux, Roman Shor, Adrian Ambrus, Parham Pournazari, Pradeepkumar Ashok, and Eric van Oort. From shallow horizontal drilling to ERD wells: How scale affects drillability and the management of drilling incidents. *Journal of Petroleum Science and Engineering*, 160(October 2017):91–105, jan 2018.

[5] Jean-Michel Coron, Rafael Vazquez, Miroslav Krstic, and Georges Bastin. Local exponential h^2 stabilization of a 2×2 quasilinear hyperbolic system using backstepping. *SIAM Journal on Control and Optimization*, 51(3):2005–2035, 2013.
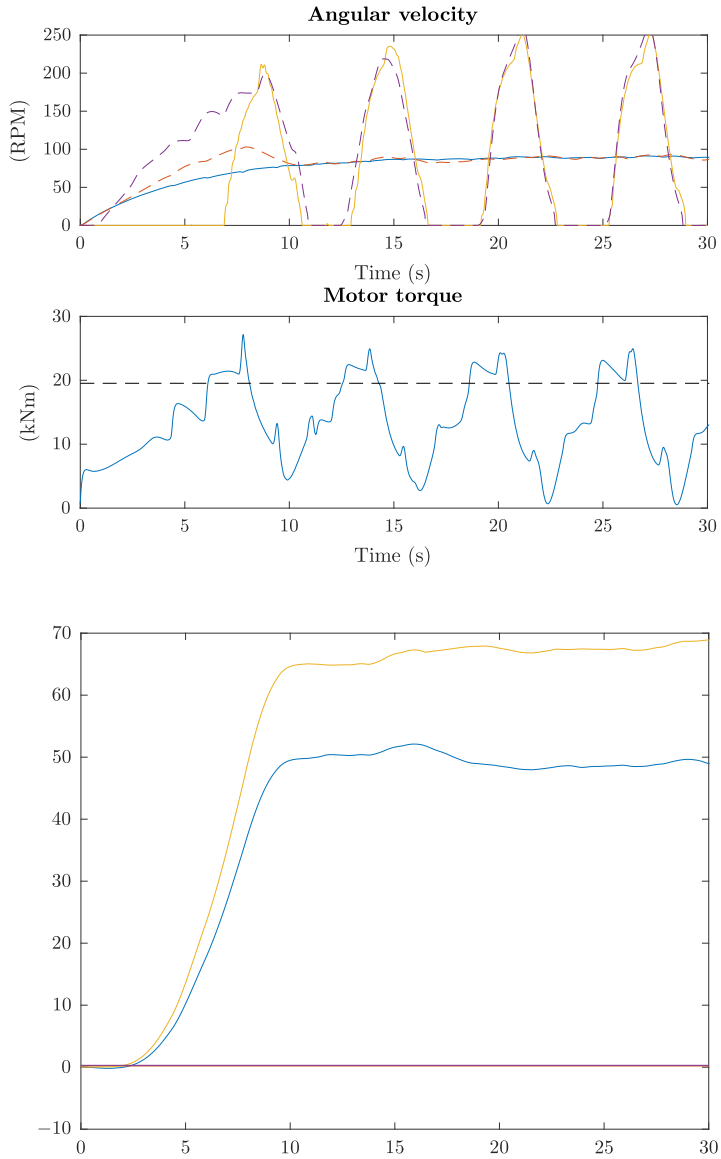
Figure 2: Plant (simulation model) and observer velocities and torque (top) and friction parameters estimates (bottom). Notice the large initial error in the latter.
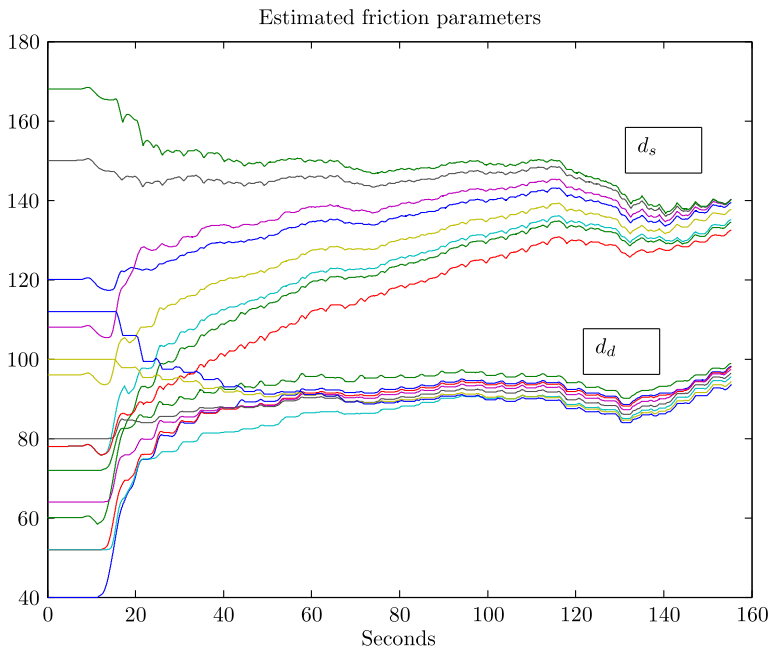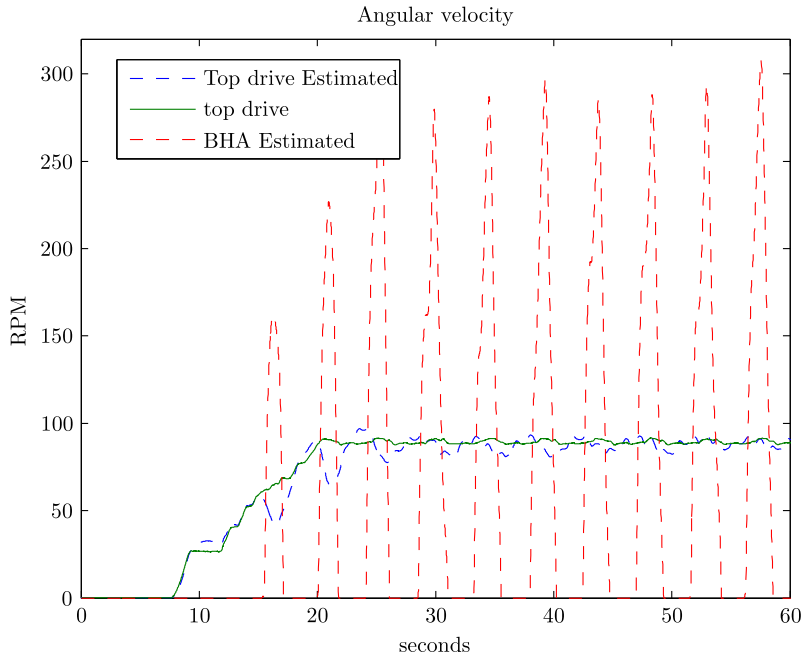
Figure 3: Plant (field data) and observer velocities and torque (top) and friction parameters estimates (bottom).

[6] Jack K Hale and Sjoerd M Verduyn Lunel. Strong stabilization of neutral functional differential equations. *IMA Journal of Mathematical Control and Information*, 19(1 and 2):5–23, 2002.

[7] Agus Hasan. Adaptive boundary control and observer of linear hyperbolic systems with application to managed pressure drilling. In *ASME 2014 Dynamic Systems and Control Conference*, pages V001T09A003–V001T09A003. American Society of Mechanical Engineers, 2014.

[8] Miroslav Krstic and Andrey Smyshlyaev. *Boundary control of PDEs: A course on backstepping designs*, volume 16. Siam, 2008.

[9] Pierre-Olivier Lamare, Jean Auriol, Florent Di Meglio, and Ulf Jakob F Aarsnes. Robust output regulation of 2 x 2 hyperbolic systems: Control law and input-to-state stability. In *American and Control Conference*, 2018.

[10] Hartmut Logemann, Richard Rebarber, and George Weiss. Conditions for robustness and nonrobustness of the stability of feedback systems with respect to small delays in the feedback loop. *SIAM Journal on Control and Optimization*, 34(2):572–600, 1996.

[11] Hector Ramirez, Hans Zwart, Yann Le Gorrec, and Alessandro Macchelli. On backstepping boundary control for a class of linear port-hamiltonian systems. In *Decision and Control (CDC), 2017 IEEE 56th Annual Conference on*, pages 658–663. IEEE, 2017.

[12] Thomas Richard, Christophe Germay, and Emmanuel Detournay. Self-excited stick-slip oscillations of drill bits. *Comptes Rendus Mécanique*, 332(8):619–626, aug 2004.

[13] Andrey Smyshlyaev and Miroslav Krstic. Closed-form boundary state feedbacks for a class of 1-d partial integro-differential equations. *IEEE Transactions on Automatic Control*, 49(12):2185–2202, 2004.

List of Participants

Bernt Sigve Aadnøy
Department of Energy and Petroleum Engineering
University of Stavanger
Stavanger Norway
bernt.aadnoy@uis.no

Ulf Jakob F. Aarsnes
International Research Institute of Stavanger
Oslo, Norway
ujfa@iris.no

Mohammad Hossein Abbasi
Centre for Analysis, Scientific Computing and Applications
Eindhoven University of Technology
Eindhoven Netherlands
m.h.abbasi@tue.nl

Adrian Ambrus
International Research Institute of Stavanger
Stavanger, Norway
Adrian.Ambrus@iris.no

Arviandy G. Aribowo
Department of Mechanical Engineering
Eindhoven University of Technology
Eindhoven, Netherlands
A.G.Aribowo@tue.nl

Bala Balachandran
Department of Mechanical Engineering
University of Maryland
College Park, MD, USA
balab@umd.edu

Bence Beri
Department of Applied Mechanics
Budapest University of Technology and Economics
Budapest, Hungary
beri@mm.bme.hu

Eric Cayeux
International Research Institute of Stavanger
Stavanger, Norway
eric.cayeux@iris.no

Shilin Chen
Halliburton Drill Bits & Services
Houston, TX, USA
Shilin.Chen@Halliburton.com

Robert Darbe
Sperry Drilling - Halliburton
Houston, TX, USA
Robert.Darbe@Halliburton.com

Emmanuel Detournay
Department of Civil Engineering
University of Minnesota
Minneapolis, MN, USA
emmanuel.detournay@gmail.com

Florent di Meglio
Centre Automatique et Systmes
MINES ParisTech
Paris, France
florent.di_meglio@mines-paristech.fr

John Morten Godhavn
Statoil
Trondheim, Norway
jmgo@statoil.com

Espen Hauge
Statoil
Trondheim, Norway
eshau@statoil.com

Sigve Hovda
Department of geoscience and petroleum
Norwegian University of Science and Technology
Trondheim, Norway
sigve.hovda@ntnu.no

Maja Ignova
Schlumberger
Cheltenham, Gloucestershire, United Kingdom
MIgnova@slb.com

Benjamin Jeffryes
Schlumberger Cambridge Research
Cambridge, United Kingdom
bpjeffryes@slb.com

Glenn-Ole Kaasa
   Kelda
   Porsgrunn, Norway
   gok@kelda.no

Julien Marck
   Sperry Drilling - Halliburton
   Houston, TX, USA
   Julien.marck@halliburton.com

Sajad Naderi
   Department of Mechanical Engineering
   Eindhoven University of Technology
   Eindhoven, Netherlands
   sj.lordejani@gmail.com

Paul Pastucek
   ExxonMobil
   Houston, TX, USA
   paul.pastusek@exxonmobil.com

Alexei Pavlov
   Department of geoscience and petroleum
   Norwegian University of Science and Technology
   Trondheim, Norway
   alexey.pavlov@ntnu.no

Greg Payette
   ExxonMobil
   Spring, TX, USA
   gregory.s.payette@exxonmobil.com

Nils Reimers
   Tomax
   Stavanger, Norway
   Nils.Reimers@tomax.no

Fahim Shakib
   Department of Mechanical Engineering
   Eindhoven University of Technology
   Eindhoven, Netherlands
   m.f.shakib@student.tue.nl

Roman Shor

Department of Chemical and Petroleum Engineering
University of Calgary
Calgary, Canada
roman.shor@ucalgary.ca

Xianfeng Song

Department of Engineering Cybernetics
Norwegian University of Science and Technology
Trondheim, Norway
xianfeng.song@ntnu.no

Dan Sui

IEP, Department of Energy and Petroleum Engineering
University of Stavanger
University of Stavanger
Stavanger, Norway
dan.sui@uis.no

Herman Y. Sutarto

Pusat Riset Energi, PT. (PRE)
East Continent Energy Indonesia (ECEI)
Jakarta, Indonesia
hytotok@gmail.com

Torstein Thingnæs

National Oilwell Varco
Stavanger, Norway
Torstein.Thingnes@nov.com

Kaixiao Tian

Department of Civil Engineering
University of Minnesota
Minneapolis, MN, USA
tianx274@umn.edu

Nathan van de Wouw

Department of Mechanical Engineering
Eindhoven University of Technology
Eindhoven, Netherlands
n.v.d.wouw@tue.nl

Naveen Velmurugan

MINES ParisTech
Paris, France
naveen.velmurugan@mines-paristech.fr

Pankaj Wahi

Department of Mechanical Engineering
Indian Institute Of Technology Kanpur
Kanpur, Uttar Pradesh
wahi@iitk.ac.in

Dapeng Zhao

Sintef
Trondheim, Norway
dapeng.zhao@sintef.no